



Available online at www.sciencedirect.com

ScienceDirect

ELSEVIER

Procedia Engineering 101 (2015) 330 – 338

**Procedia
Engineering**

www.elsevier.com/locate/procedia

3rd International Conference on Material and Component Performance under Variable Amplitude Loading, VAL2015

Fatigue Damage Comparison of Mechanical Components in a Land-Based and a Spar Floating Wind Turbine

Amir Rasekhi Nejad^{a,b,*}, Erin E. Bachynski^{b,c}, Zhen Gao^{a,b}, Torgeir Moan^{a,b}

^aNorwegian Research Centre for Offshore Wind Technology (NOWITECH)

^bCentre for Ships and Ocean Structures (CeSOS) & Centre for Autonomous Marine Operations and Systems (AMOS),

Norwegian University of Science and Technology (NTNU)

^cMARINTEK, Trondheim, Norway

Abstract

This paper investigates the fatigue damage of the gears and bearings in a land-based and a spar-type floating wind turbine. The reference 5 MW NOWITECH gearbox is used on a land-based and a floating spar wind turbine. First, the global analysis is carried out in an aero-hydro-servo-elastic code. Next, the forces, moments and motions from the global analysis are applied to the gearbox modelled in a Multi Body Simulation (MBS) and forces on gears and bearings are obtained. The fatigue damage is then calculated based on the SN-curve approach and Palmgren-Miner linear damage hypothesis in an identical wind condition and compared for both turbines.

© 2015 The Authors. Published by Elsevier Ltd. This is an open access article under the CC BY-NC-ND license (<http://creativecommons.org/licenses/by-nc-nd/4.0/>).

Peer-review under responsibility of the Czech Society for Mechanics

Keywords: Gear; Bearing; Fatigue; Offshore Wind Turbines; Floating Wind Turbines; Spar

1. Introduction

Wind energy harvesting from the offshore environment is attractive due to, among others, the steady wind conditions and high mean wind speed. In the last decade, in addition to shallow water bottom-fixed wind turbines, floating wind turbines have been in the centre of research and development. Hywind, the first floating wind turbine

* Corresponding author. Tel.: +47-735-91546; fax: +47-735-95528.

E-mail address: Amir.Nejad@ntnu.no

prototype, was installed in 2009 off the coast of Norway and the second one, WindFloat, in 2011 in Portugal. Many studies have been dedicated to the structural load and load response analysis of floating wind turbines [1-4], but few have been focused on the mechanical components and drivetrains. One of the first studies on floating vs. fixed wind turbine drivetrains was carried by Xing et al. [5], where the higher load variations on the drivetrain of a spar type wind turbine were identified. In fatigue analysis, Dong et al. [6], Nejad et al. [7] or Jiang et al. [8] have investigated the gear contact fatigue, gear tooth root bending fatigue and bearing contact fatigue in wind turbine gearboxes. However, all these fatigue studies have employed land-based or bottom-fixed wind turbines, and not floating turbines.

Drivetrains with gears are still the dominant technology for wind turbines with market share of more than 85% [9]. In this paper, the 5 MW reference gearbox [10] with conventional three stage gears is used for fatigue damage comparison of a land-based and a spar wind turbines. The fatigue damage of gears and bearings is compared at the rated wind speed.

2. Methodology

2.1. Decoupled analysis

A decoupled analysis method is used to estimate the drivetrain dynamic load response from the environmental loads - see Figure 1 - and next, the forces, moments and motions from the global analysis are applied to the gearbox modelled in a Multi Body Simulation (MBS) and forces on gears and bearings are obtained.

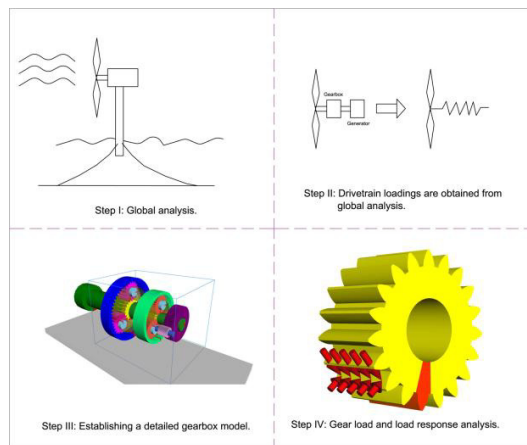


Fig. 1. Decoupled approach for wind turbine gearbox analysis.

The global analysis is conducted by using an aero-hydro-servo-elastic code, SIMO-RIFLEX-AeroDyn [11]. Simulations are carried out for mean wind speed 12 m/s, which is close to the rated wind speed of 11.4 m/s. According to Nejad et al. [7] the rated wind speed holds the highest contribution in the gear fatigue damage, therefore the fatigue damage near the rated wind speed is compared for the land-based and the spar wind turbine. For the spar wind turbine, simulations are carried out at the rated wind speed with wave conditions characterized by significant wave height $H_s = 5$ m and peak period $T_p = 12$ s (modelled by a JONSWAP spectrum). The turbulence intensity factor is taken as 0.15 according to IEC 61400-1 [12] for both the spar and land-based turbines.

To minimize the statistical uncertainties, six 3800s simulations are carried out for each wind speed. The first 200 s are removed during post-processing to avoid start-up transient effects. More information about the decoupled approach and its limitations can be found in [6,7,13,14].

2.2. Fatigue damage comparison in gears

Among the many failure modes of gears, the gear tooth root bending fatigue failure can cause particularly catastrophic consequences and total damages [15]. The short-term gear tooth root bending fatigue damage can be estimated by the Palmgren-Miner hypothesis of linear damage and SN curve data [7]:

$$D = \frac{N_T}{K_C} a^m \Gamma \left(1 + \frac{m}{c} \right) \quad (1)$$

where N_T is the number of stress cycle in one hour, K_C and m are SN curve parameters and a, c are the Weibull shape and scale parameters of stress range in the form of:

$$F_s(s) = 1 - \exp \left(- \left(\frac{s}{a} \right)^c \right) \quad (2)$$

The stress range is obtained by the load duration distribution (LDD) method [16]. In every rotation, a single tooth undergoes root bending or surface pitting stress ranging from zero to a certain peak value which does not explicitly correspond to the input load fluctuations. This is due to the fact that the gear stress range is not only a function of the external load fluctuations but also a function of gear rotational speed. In wind turbines, the stress range for different gear stages should be established by taking into account both load and speed variations. Therefore, the stress cycle counting method for gears is not the same as for structural components. More information about this method and gear tooth root fatigue calculation can be found in Nejad et. al [7].

2.3. Fatigue damage comparison in bearings

The bearing life and damage calculation is generally based on the Lundberg-Palmgren [17] equation:

$$\frac{1}{PL^a} = C \quad (3)$$

where L is the bearing basic life, defined as the number of cycles that 90% of an identical group of bearings achieves, under a certain test conditions, before the fatigue damage appears. P is the dynamic equivalent radial load calculated from $P = XF_r + YF_a$, and F_a, F_r are the axial and radial loads on the bearing respectively, X, Y are constant factors provided by manufacturers. a is 3 for ball bearing and 3.33 for roller bearings. C is the basic load rating and constant for a given bearing.

Equation (3) is one form of the single SN curve formulation. Comparing this equation with Palmgren-Miner's hypothesis of linear cumulative damage, the damage is obtained by [15]:

$$D = \sum_i \frac{l_i}{L_i} = \frac{1}{C^a} \sum_i l_i P_i^a \quad (4)$$

where D is the fatigue damage for a load with duration of 1 hour and l_i is the number of load cycles in 1 hour associated with load range P_i . It should be noted that the method described herein is the most common approach for bearing life calculation. More refined methods considering internal components can be found in Jiang et al. [8].

3. Land-based and spar wind turbine models

The NREL 5MW reference wind turbine [18] is studied in both the original land-based configuration and mounted on the floating OC3 Hywind hull [19]. The reference turbine is a 3-bladed upwind turbine with rated speed 12.1 rpm. Both are modelled in SIMO-RIFLEX-AeroDyn, which consists of three integrated simulation tools. SIMO models the rigid body hydrodynamics of the hull and rigid body components of the turbine (nacelle and hub); RIFLEX, includes the finite element solver, the flexible beam elements, and the link to an external controller; and AeroDyn provides the forces and moments on the blades based on Blade Element/Momentum (BEM) or Generalized Dynamic Wake (GDW) theories, including dynamic stall, tower shadow, and skewed inflow correction [20]. The generator torque and blade pitch control system was written in Java. This combination provided a stable nonlinear finite element solver, sophisticated hydrodynamics, well-tested aerodynamics, and control logic.

The spar hull was modeled as a rigid body, while the tower, blades, and mooring lines consisted of flexible components. A chain mooring system with delta lines and clump weights was applied to approximate the mooring system stiffness described by Jonkman [19]. The mooring lines were modeled using bar elements and connecting joints, allowing for a full dynamic solution. Additional information about the model is given by Bachynski et al. [4].

The models are shown in Figure 2 and their general characteristics are summarized in Table 1.

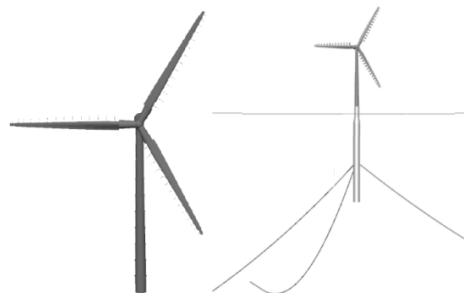


Fig. 2. Land-based (left) and spar wind turbines modelled in SIMA. Note that the full extent of the spar mooring system is not shown.

Table 1. General characteristics of the modelled wind turbines.

	Land-based turbine	Spar wind turbine
Hub height	90 m	90 m
Tower length	87.6 m	77.6 m
Key natural periods	1 st tower fore-aft: 3.1 s 2 nd tower fore-aft: 0.4 s	Platform surge: 129.5 s Platform pitch: 29.7 s Platform yaw: 8.2 s 1 st tower fore-aft: 2.1 s
Controller natural frequency	0.6 rad/s	0.2 rad/s

4. 5 MW gearbox model

The 5 MW reference gearbox for offshore wind turbines developed by NOWITECH has been used in this study [10]. This gearbox consists of three stages, two planetary gears and one parallel helical gears. The general specification of the gearbox is listed in Table 2.

Table 2. 5 MW gearbox model specification [10].

Parameter	Value
1 st stage ratio	1:3.947
2 nd stage ratio	1:6.167
3 rd stage ratio	1:3.958
Total ratio	1:96.354
Power (kW)	5000
Rated input shaft speed (rpm)	12.1
Rated input shaft torque (kN-m)	3946

As it is shown in the layout and topology Figures 3 and 4, gearbox is fitted with two main bearings to reduce the non-torque loadings on gear stages. Components' designations are also illustrated in Figure 4.

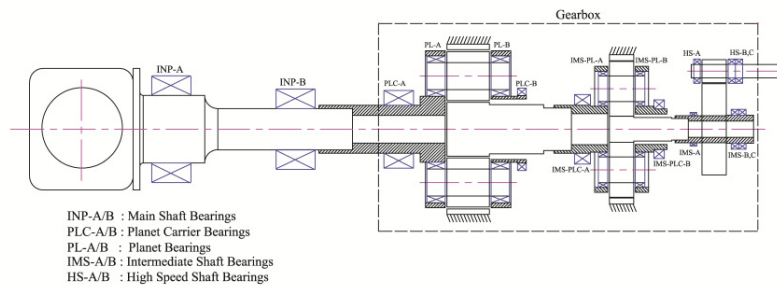


Fig. 3. 5 MW reference gearbox schematic layout.

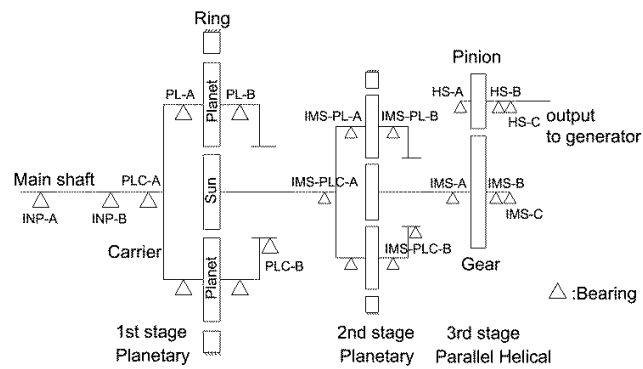


Fig. 4. 5 MW gearbox topology and components' designations.

The MBS model of the 5 MW reference gearbox is shown in Figure 5.

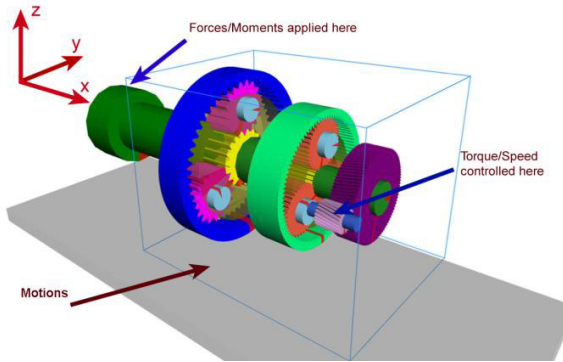


Fig. 5. 5 MW gearbox MBS model.

5. Results and discussions

The fatigue damage in gears and bearings for land-based and spar wind turbines is compared by a comparison factor in percentage, χ , defined as:

$$\chi = \frac{D_{sp} - D_{lb}}{D_{lb}} \times 100 \quad (5)$$

where D_{lb}, D_{sp} are fatigue damage in land-based and spar respectively. The bearings and gears selected for comparisons are chosen based on the fatigue damage ranking map – vulnerability map – as described in reference [15]. Figure 6 shows the vulnerability map for the 5 MW reference gearbox. In this map, the gears and bearings are highlighted based on their fatigue damage rankings.

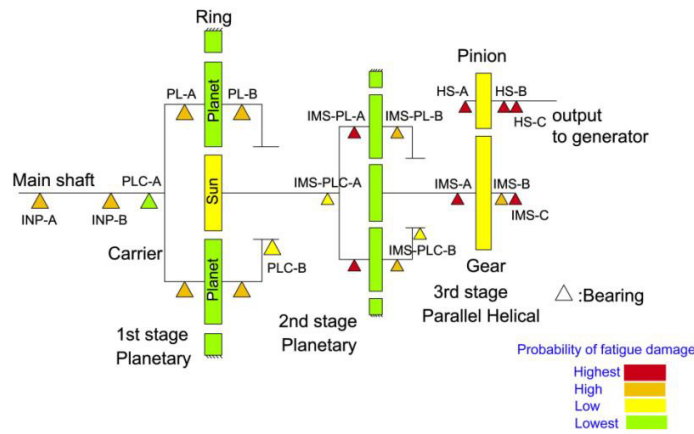


Fig. 6. 5 MW gearbox vulnerability map [10].

Table 3 presents the fatigue damage comparison factor, χ , as defined in equation (5).

Table 3. Fatigue damage comparison factor, χ %.

Bearing/gear designation	Description	χ %
INP-A	Main bearing, upwind	-19
INP-B	Main bearing, downwind	+200
PL-A	1 st stage, planet bearing, upwind	0
PL-B	1 st stage, planet bearing, downwind	-4
IMS-PL-A	2 nd stage, planet bearing, upwind	0
IMS-PL-B	2 nd stage, planet bearing, downwind	-2
IMS-C	Bearing on medium speed shaft	-1
HS-C	Bearing on high speed shaft	-4
1 st stage sun gear	1 st stage sun gear	-2
3 rd stage pinion	3 rd stage pinion	-3

In Table 3, the negative values indicate lower damage in spar type floating wind turbine, while positive means higher damage. As it is shown, most of the components encounter lower damage in spar type wind turbine, except the second main bearing (INP-B) which faces damages around two times more than in land-based turbine. The first main bearing (INP-A) is designed to carry the radial loads while INP-B carries both radial and axial loads. As it is presented in Figure 7(a), the axial load variation on INP-B in spar is higher than in the land-based gearbox. Moreover, the bearing fatigue damage is a function of equivalent load range on power of 3.33 – see equation (4). The equivalent load for the INP-B is obtained from $P = 0.67F_r + 3.6F_a$, thus even a small increase in axial force range causes a considerable bearing damage. It should be noted that both spar and land-based turbine produce the same mean power – Figure 7(b).

The results also show that the upwind planet bearing sustains higher damage than the downwind bearing in the spar drivetrain. This is in line with the results found in earlier studies of land-based gearboxes [21,22].

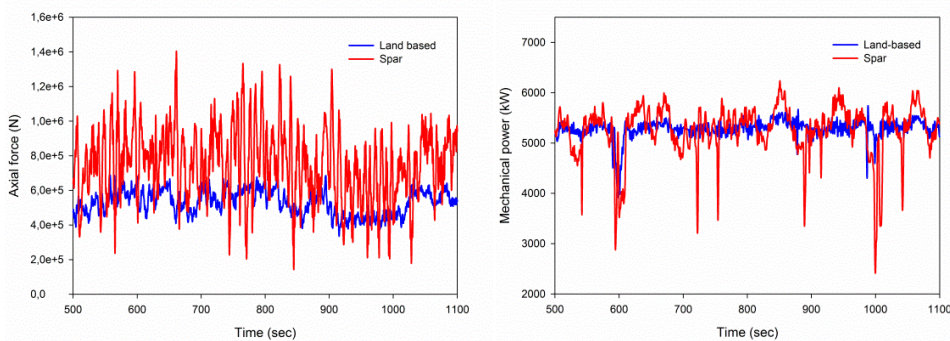


Fig. 7. Left (a): axial force on 2nd main bearing (INP-B), land-based and spar. Right (b): mechanical power, land-based and spar.

6. Conclusions

In this paper the fatigue damage of gears and bearings of a spar type wind turbine is compared with a land-based turbine. A reference 5 MW gearbox modeled by multibody simulation is employed for both land-based and spar wind turbines. The global analysis is carried at same wind condition for both wind turbines, while the representative correlated wave is also applied on the spar. The forces, movements and motions obtained from the global analysis are then applied on the gearbox in multibody model. From the multibody outputs, the fatigue damage of gears and bearing are calculated.

It is found that the main bearing carrying axial loads sustains higher damage in spar than the land-based turbine. Other gears and bearings encounter lower or equal damages in spar turbine comparative with the land-based. Moreover, it is highlighted that the bearing life is unequal for upwind and downwind planet bearings in spar wind turbine similar to the land-based turbine.

Acknowledgements

The authors wish to acknowledge the financial support from Research Council of Norway through Norwegian Research Centre for Offshore Wind Technology (Nowitech) and Centre for Ships and Ocean Structures (CeSOS).

References

- [1] Moan T., Gao Z., Karimirad M., Bachynski E. E., Etemaddar M., Jiang Z., Kvitem M. I., Muliawan M., and Xing Y. Recent Developments of the Design and Analysis of Floating Wind Turbines, in ISCOT: Developments In Fixed & Floating Offshore Structures, 2012.
- [2] Jonkman J., and Matha D. A Quantitative Comparison of the Responses of Three Floating Platforms, in European Offshore Wind 2009 Conference and Exhibition, 2009.
- [3] Cordle A., and Jonkman J. State of the Art in Floating Wind Turbine Design Tools', in Proceedings of the Twenty-first (2011) International Offshore and Polar Engineering Conference, 2011.
- [4] Bachynski, E.E., Kvitem, M.I., Luan, C., Moan, T., 2014. Wind-wave misalignment effects on floating wind turbines: motions and tower load effects. *Journal of Offshore Mechanics and Arctic Engineering*; volume 136, pp. 041902-1-- 041902-12. doi:10.1115/1.4028028.
- [5] Xing Y., Karimirad M. and Moan, T. Modelling and analysis of floating spar-type wind turbine drivetrain. *Wind Energy*, 17: 565–587, 2014.
- [6] Dong W., Xing Y., Moan T., and Gao Z. Time domain-based gear contact fatigue analysis of a wind turbine drivetrain under dynamic conditions. *International Journal of Fatigue*, 48:133–146, 2013.
- [7] Nejad A.R., Gao Z., and Moan T. On long-term fatigue damage and reliability analysis of gears under wind loads in offshore wind turbine drivetrains. *International Journal of Fatigue*, 61:116–128, 2014.
- [8] Jiang Z., Xing Y., Guo Y., Moan T., and Gao Z. Long-term contact fatigue analysis of a planetary bearing in a land-based wind turbine drivetrain. *Wind Energy*. doi: 10.1002/we.1713.
- [9] Kaldellis J.K. and Zafirakis D.P. Trends, prospects and R & D directions in wind turbine technology. In Ali Sayigh (eds.), *Comprehensive Renewable Energy*, 671–724, Elsevier, 2012.
- [10] Nejad A.R., Guo Y., Gao Z., and Moan T. Development of a 5 mw reference gearbox for offshore wind turbines. *Wind Energy*, submitted for publication, 2014.
- [11] Ormberg, H., and Bachynski E. E. Global Analysis of Floating Wind Turbines: Code Development, Model Sensitivity, and Benchmark Study. Proceedings of the 22nd International Offshore (Ocean) and Polar Engineering Conference, Rhodes, Greece, June 2012. 2012-TPC-0734.
- [12] IEC 61400-1. Wind turbines, part 1: Design requirements, 2005.
- [13] Nejad A.R., Gao Z., and Moan T. Long-term analysis of gear loads in fixed offshore wind turbines considering ultimate operational loadings. *Energy Procedia*, 35:187–197, 2013.
- [14] Nejad A.R., Xing Y., and T. Moan. Gear train internal dynamics in large offshore wind turbines. In ASME 2012 11th Biennial Conference on Engineering Systems Design and Analysis, pages 823–831. American Society of Mechanical Engineers, 2012.
- [15] Nejad A.R., Gao Z., and Moan T. Fatigue reliability-based inspection and maintenance planning of gearbox components in wind turbine drivetrains. *Energy Procedia*, 53:248–257, 2014.
- [16] IEC 61400-4. Wind turbines, part 4: Standard for design and specification of gearboxes, 2012.
- [17] Lundberg G. and Palmgren A. Dynamic capacity of rolling bearings. *Acta Polytechnica Mechanical Engineering Series*, 2:5–32, 1952.
- [18] Jonkman, J., Butterfield, S., Musial, W., and Scott, G. Definition of a 5-MW Reference Wind Turbine for Offshore System Development. 2009, National Renewable Energy Laboratory. NREL/TP-500-38060
- [19] Jonkman, J., Definition of the Floating System for Phase IV of OC3. 2010. NREL/TP-500-47535.
- [20] Moriarty, P.J. and Hansen A.C., AeroDyn Theory Manual. 2005. NREL/TP-500-36881.

- [21] LaCava W., Keller J., and McNiff B. Gearbox reliability collaborative: test and model investigation of sun orbit and planet load share in a wind turbine gearbox. National Renewable Energy Laboratory, NREL/CP-5000-54618, 2012.
- [22] Nejad A. R., Xing Y., Guo Y., Keller J., Gao Z., and Moan T. Effects of floating sun gear in a wind turbine's planetary gearbox with geometrical imperfections, Wind Energy, 2014, doi: 10.1002/we.1808.